

## ORIGINAL RESEARCH ARTICLE

# Correspondence between theory and practice of a Beerkan infiltration experiment

Vincenzo Bagarello<sup>1</sup>  | Michal Dohnal<sup>2</sup>  | Massimo Iovino<sup>1</sup>  | Jianbin Lai<sup>3</sup> 

<sup>1</sup>Dep. of Agricultural, Food and Forest Sciences, Univ. of Palermo, Viale delle Scienze bldg. 4, Palermo 90128, Italy

<sup>2</sup>Dep. of Hydraulics and Hydrology, Czech Technical Univ. in Prague, Prague 6, 166 29, Czech Republic

<sup>3</sup>Yucheng Comprehensive Experimental Station, Institute of Geographic Sciences and Natural Resources Research, Chinese Academy of Sciences, Beijing 100101, China

## Correspondence

Jianbin Lai, Yucheng Comprehensive Experimental Station, Institute of Geographic Sciences and Natural Resources Research, Chinese Academy of Sciences, Beijing, 100101, China.

Email: [laijianbin@igsnr.ac.cn](mailto:laijianbin@igsnr.ac.cn)

Assigned to Associate Editor Zhuanfang Zhang.

## Abstract

The Beerkan infiltration experiment is carried out by inserting the ring a short depth into the soil and establishing a positive head of water on the infiltration surface for at least a part of the run. Nevertheless, the data are analyzed by assuming a fully unconfined infiltration process (ring insertion depth,  $d = 0$  cm) and a null ponded depth of water ( $H = 0$  cm). The influence of ring insertion and ponded water on an infiltration process of 2 h sampled every minute was tested in this numerical investigation. Five soils varying from sand to silt loam, three ring radii (5–15 cm), and the Beerkan-specific range of values for both  $d$  and  $H$  (between 0 and 1 cm) were considered. The differences between the theoretical ( $d = H = 0$  cm) and the practical ( $d = H = 1$  cm) setups varied from  $-10.4$  to  $+8.6\%$  for the mean infiltration rate and from  $-10.2$  to  $+8.3\%$  for the final cumulative infiltration. These differences were small, and they decreased in absolute value by considering a soil-dependent ring radius. In particular, nearly negligible differences were detected using a small ring in coarse-textured soils and a large ring in fine-textured soils. In the coarser soils, inserting the ring and establishing a ponded depth of water did not alter the estimated coefficients of the two-parameter infiltration model appreciably with the cumulative linearization method, because these coefficients differed between the theoretical and practical setups by no more than 9.2%. In fine soils, linearization could not be possible regardless of the considered setup, or it was the use of  $d = H = 1$  cm instead of  $d = H = 0$  cm that impeded a convincing linearization of the data. In conclusion, the good correspondence, in many circumstances, between the theoretical and the practical Beerkan infiltration experiment reinforced the interest in this simple experiment as a practical means to collect infiltration data in the field.

**Abbreviations:** L, loam; LS, loamy sand; 1D, one dimensional; Ssand, sand; SAL, sandy loam; SIL, silt loam; 3D, three dimensional.

This is an open access article under the terms of the [Creative Commons Attribution](https://creativecommons.org/licenses/by/4.0/) License, which permits use, distribution and reproduction in any medium, provided the original work is properly cited.

© 2022 The Authors. *Vadose Zone Journal* published by Wiley Periodicals LLC on behalf of Soil Science Society of America.

## 1 | INTRODUCTION

The correspondence between theory and practice, an obvious prerequisite of any experimental data analysis procedure, has to be guaranteed when soil hydrodynamic parameters are estimated from single-ring infiltration data.

The physically based infiltration model by Haverkamp et al. (1994) has been widely used for the theoretical description of three-dimensional (3D) infiltration from a circular source into an initially unsaturated soil. This model was specifically developed to analyze disc, or tension, infiltrometer experiments (i.e., 3D processes under a pressure head not greater than zero). Therefore, the use of the model to deduce the saturated soil hydrodynamic parameters is limited to fully unconfined infiltration experiments (ring insertion depth,  $d = 0$  cm) with a null ponded depth of water on the infiltration surface ( $H = 0$  cm).

However, experimental data are frequently obtained by the so-called Beerkan infiltration run (Lassabatere et al., 2006). This experiment agrees only approximately with the theoretical assumptions of the infiltration model by Haverkamp et al. (1994), because the ring used to confine the infiltration surface is inserted into the soil to a short depth to avoid lateral loss of water during the run. In addition, repeatedly pouring a small water volume into the ring determines a positive pressure head on the soil surface for at least a part of the experiment. A variety of setups can be found with reference to the used  $d$  and  $H$  values. For example, Lassabatere et al. (2006) inserted the ring to a depth of about 1 cm, and the initial ponded depth of water was 0.2–0.8 cm, depending on the run. A ring inserted 1 cm into the soil and an initial ponded depth of water of nearly 1 cm were reported by Xu et al. (2012) and Lozano-Baez et al. (2021), whereas a ring insertion depth of 2 cm was reported by Hoeffner et al. (2021). The automated single-ring infiltrometer by Di Prima (2015) maintains a small (i.e., approximately less than 0.5 cm) water head on the confined soil surface. Therefore, the practice does not generally agree with the theory, because a repeated falling-head process is considered similar to a constant-head process and  $d$  and  $H$  values are greater than zero. On the other hand, the vast majority of  $d$  and  $H$  values do not exceed 1 cm.

The similarity between a falling-head and a constant-head process for boundary conditions similar to a Beerkan infiltration run was suggested by Touma et al. (2007) using numerically obtained infiltration data. However, these authors did not consider the case of a steadily null ponded depth of water on the infiltration surface, because numerical tests performed by allowing ponded depth of water to vary from 0.68 to 0 cm were compared with those obtained with a constant depth of water of 0.34 cm. Numerical simulations were also used in other investigations to test different  $H$  and  $d$  effects on infiltration. In particular, Dušek et al. (2009) showed that a higher water level in the ring produces higher infiltration rates

### Core Ideas

- Beerkan infiltrations were conducted under both theoretical and practical conditions.
- Five soils and three ring radii were considered in verifying the correspondence of infiltration characteristics.
- The differences of infiltration rate and cumulative infiltration between theoretical and practical infiltration were minor.
- The practical interest was reinforced for the Beerkan infiltration as a simple method to collect infiltration data.

due to a greater pressure gradient and that infiltration rates decrease as  $d$  increases, because flow moves from a purely 3D process for  $d = 0$  cm to a combination of one-dimensional (1D) and 3D processes for  $d > 0$ . Dohnal et al. (2016) later showed that the transition from the vertical 1D flow within the infiltration ring to 3D flow below the ring implies the appearance of an initial bend when the linearization method by Vandervaere et al. (2000a) is applied. However, the results obtained by Dušek et al. (2009) and Dohnal et al. (2016), referring to  $d$  values of  $\geq 5$  cm, are not directly applicable to a Beerkan infiltration experiment because there is no evidence that a small ring insertion depth has the same practical effects as a deeper insertion. Thus, the available information on the  $H$  and  $d$  effects on infiltration is incomplete. In particular, it is still necessary to test the influence of the ring insertion depth and the established ponded depth of water on the infiltration process by considering different soils and the Beerkan-specific range of values for these two variables. More precisely, the level of agreement between a real ( $d$  and  $H$  close to 1 cm) and the theoretical ( $d = H = 0$  cm) Beerkan infiltration run has to be assessed. Numerical simulation of the infiltration process appears appropriate for testing hypotheses and checking factors that can be expected to affect a particular procedure to estimate soil parameters because a numerical experiment can be performed in fully controlled conditions and it is not hampered by experimental errors (e.g., Bagarello et al., 2019; Lai et al., 2010; Lai & Ren, 2007; Reynolds, 2013; Wu et al., 1993).

The general objective of this investigation was to verify if a Beerkan infiltration experiment can be considered appropriate for an analysis that assumes a fully unconfined process under a null ponded depth of water. With reference to five soils differing by their characteristics, the specific objective was to determine both the separate and the combined effects of a small ponded depth of water on the infiltration surface and a small ring insertion depth on (a) infiltration

rate, (b) cumulative infiltration, and (c) linearized cumulative infiltration.

## 2 | THEORY

The two-parameter infiltration equation is written as (Philip, 1957):

$$I = C_1 t^{1/2} + C_2 t \quad (1)$$

where  $I$  [L] is the cumulative infiltration,  $t$  [T] is the time, and  $C_1$  [ $L T^{-1/2}$ ] and  $C_2$  [ $L T^{-1}$ ] are coefficients having a physical meaning in the simplified time expansion by Haverkamp et al. (1994). In particular, the first term of Equation 1 indicates vertical capillarity, whereas the second term refers to gravity and lateral capillarity during the 3D infiltration process (Vandervaere et al., 2000b). According to Smiles and Knight (1976) and Vandervaere et al. (2000a), the adequacy of the two-term equation with the data can be checked by the so-called cumulative linearization method in which both sides of Equation 1 are divided by  $t^{1/2}$ :

$$\frac{I}{t^{1/2}} = C_1 + C_2 t^{1/2} \quad (2)$$

If we understand Equation 2 as a straight-line equation, the infiltration data can be plotted on a  $I/t^{1/2}$  against  $t^{1/2}$  graph where  $C_1$  and  $C_2$  appear as the intercept and the slope of the linear regression line, respectively.

## 3 | MATERIALS AND METHODS

### 3.1 | Soils and numerical experiments

Five soils—namely, sand (S), loamy sand (LS), sandy loam (SAL), loam (L), and silt loam (SIL)—were considered in this study. These soils were chosen because they differed widely by their hydraulic properties, allowing exploration of a wide range of situations. Soil hydraulic properties were determined according to the van Genuchten–Mualem model (Mualem, 1976; van Genuchten, 1980) with hydraulic parameters adopted from Carsel and Parrish (1988) (Table 1).

Infiltration experiments were numerically conducted by considering homogeneous soil conditions and using HYDRUS-2D/3D (Šimůnek et al., 2007), which was demonstrated to be a robust and reliable tool for simulating water flow in the soil under various conditions (Šimůnek et al., 2016; Varvaris et al., 2021). The modeling comprised three-dimensional axisymmetric simulations. To guarantee an unrestricted flow, the size of the flow domain was 80 cm in  $X$  and 100 cm in  $Z$  for the L and SIL soils, whereas it was 100 cm in  $X$  and 200 cm in  $Z$  for the S, LS and SAL soils. The element size was 0.05 cm for the upper 10 cm of the flow domain, and then it gradually increased to 5 cm at the bottom.

A variable density of element mesh was chosen to ensure the simulation accuracy for a relatively large flow domain. The boundary condition at the bottom was free drainage, and no lateral flux was considered for the vertical boundaries of the simulation domain. An upper boundary condition of constant water head was assigned within the ring to simulate infiltration under ponding conditions.

For each soil, three radii of the infiltration ring were considered (i.e.,  $r = 5, 10,$  and  $15$  cm). For each ring radius, two ring insertion depths (i.e.,  $d = 0$  cm and  $d = 1$  cm) and two ponding heads (i.e.,  $H = 0$  and  $1$  cm) were used in this study. Therefore, 12 combinations (3 ring radii  $\times$  2 ring insertion depths  $\times$  2 ponding heads) were considered for each soil.

The initial condition was set to be a uniform water pressure head within the whole flow domain. For each simulation with the four setups, that is,  $d = H = 0$  cm (d0H0),  $d = 1$  cm and  $H = 0$  cm (d1H0),  $d = 0$  cm and  $H = 1$  cm (d0H1), and  $d = H = 1$  cm (d1H1), the initial volumetric soil water content,  $\theta_i$  [ $L^3 L^{-3}$ ], was set equal to 0.25 (25%) of the saturated volumetric water content,  $\theta_s$  [ $L^3 L^{-3}$ ], for each soil type (Table 1). This choice was made taking into account that (a) Lassabatere et al. (2006) did not recommend  $\theta_i/\theta_s > 0.25$  for determining the soil hydrodynamic parameters with the Haverkamp et al. (1994) model, and (b) excessively dry or wet soil conditions, even if they can persist for long times in certain environments, are not recommended for performing single-ring infiltration experiments for practical reasons, including shattering (dry soil) or compaction (wet soil) risks associated with ring insertion (Reynolds, 1993). Nevertheless, control simulations with the d0H0 and d1H1 setups were also performed for  $\theta_i/\theta_s = 0.20$  and  $0.30$  (Table 1) and the two limit values of  $r$  (5 and 15 cm) to detect a possible dependence of the setup effects on the antecedent soil water content in a range of wetness conditions having some practical interest.

The infiltration duration was 2 h for all simulation runs, in accordance with Dušek et al. (2009) and considering that this duration represents a plausible time limit for a field run in many circumstances. Flow was not affected by the established boundaries of the domain during the simulation period. Therefore, the setting of the simulation domain was appropriate to represent the actual infiltration process under the various considered setups.

Cumulative infiltration,  $I$  [L], and instantaneous infiltration rate,  $i_r$  [ $L T^{-1}$ ], were sampled every minute to obtain, for each simulation, cumulative infiltration and infiltration rate curves composed of 120 data points.

Single-ring infiltration data are frequently used to determine soil hydrodynamic parameters by infiltration models that are strictly usable in ideal porous media (i.e., homogeneous, rigid, and isotropic). Therefore, simulated infiltration was consistent, from a theoretical point of view, with the use of the data for characterization of the soil hydrodynamic behavior.

TABLE 1 Soil hydraulic parameters (Carsel &amp; Parrish, 1988) and initial conditions in simulations

Soil	van Genuchten–Mualem parameters					Initial conditions					
						$\theta_r/\theta_s = 0.20$		$\theta_r/\theta_s = 0.25$		$\theta_r/\theta_s = 0.30$	
	$\theta_r$	$\theta_s$	$\alpha$	$n$	$K_s$	$h_i$	$\theta_i$	$h_i$	$\theta_i$	$h_i$	$\theta_i$
Sand	0.045	0.43	0.145	2.68	$8.25 \times 10^{-3}$	-25.9	0.086	-19.9	0.108	-16.5	0.129
Loamy sand	0.057	0.41	0.124	2.28	$4.05 \times 10^{-3}$	-63.6	0.082	-39.5	0.103	-29.2	0.123
Sandy loam	0.065	0.41	0.075	1.89	$1.23 \times 10^{-3}$	-392.2	0.082	-161.0	0.103	-97.7	0.123
Loam	0.078	0.43	0.036	1.56	$2.88 \times 10^{-4}$	-23,901.6	0.086	-2,323.0	0.108	-872.1	0.129
Silt loam	0.067	0.45	0.020	1.41	$1.25 \times 10^{-4}$	-47,659.3	0.090	-9,022.0	0.113	-3,381.5	0.135

Note.  $\theta_r$  ( $\text{cm}^3 \text{cm}^{-3}$ ) = residual volumetric soil water content;  $\theta_s$  ( $\text{cm}^3 \text{cm}^{-3}$ ) = saturated volumetric soil water content;  $\alpha$  ( $\text{cm}^{-1}$ ) and  $n$  = empirical parameters of the van Genuchten (1980) model for the water retention curve;  $K_s$  ( $\text{cm s}^{-1}$ ) = saturated soil hydraulic conductivity;  $h_i$  (cm) = initial soil water pressure head;  $\theta_i$  ( $\text{cm}^3 \text{cm}^{-3}$ ) = initial volumetric soil water content.

### 3.2 | Data analysis

Dependence of setup effects on the antecedent soil water content was initially tested by determining, for each soil (S, LS, SAL, L, and SIL), ring radius ( $r = 5$  and  $15$  cm) and  $\theta_r/\theta_s$  ratio (0.20, 0.25, and 0.30), the percentage difference,  $\Delta i_r$  (%), between the instantaneous infiltration rate for the d1H1 setup, and the corresponding  $i_r$  value for the d0H0 setup. Therefore, a total of 3,600  $\Delta i_r$  values (5 soils  $\times$  2 radii  $\times$  3  $\theta_r/\theta_s$  values  $\times$  120  $i_r$  values during a run) were calculated. A comparison was then performed among the three  $\Delta i_r$  values obtained with the three antecedent soil water conditions for given soil, radius, and time. A similarity of the three  $\Delta i_r$  values suggested that  $\theta_r/\theta_s$  did not appreciably influence the difference between the theoretical (d0H0) and the practical (d1H1) setups. Instead, large  $\Delta i_r$  differences indicated that the setup effects varied with the antecedent soil water content. The same procedure was applied for the cumulative infiltration at the end of the 2-h period,  $I_{2h}$  [L]. In this case, the relative difference was denoted as  $\Delta I_{2h}$  (%), and a total of 30  $\Delta I_{2h}$  values (5 soils  $\times$  3  $\theta_r/\theta_s$  values  $\times$  2 ring radii) were considered.

Further analyses were performed with reference to the  $\theta_r/\theta_s = 0.25$  antecedent soil water condition. In particular, for each soil and ring radius, the infiltration rate, normalized with respect to  $K_s$  [ $\text{L T}^{-1}$ ], was plotted against time,  $t$  [T], for the four considered setups (i.e., d0H0, d1H0, d0H1, and d1H1). The effect of using larger  $d$  and  $H$  values than the theoretical null values was also examined by calculating the percentage difference,  $\Delta i_r$  (%), between the instantaneous infiltration rates corresponding to the d1H0, d0H1, and d1H1 setups and those obtained for the d0H0 setup. The same procedure was applied for  $I_{2h}$  by calculating  $\Delta I_{2h}$  (%).

There are no shared guidelines that could help to judge the similarity of infiltration rates, and comparisons are often qualitative or only report percentage differences between corresponding values (Dušek et al., 2009; Wu et al., 1997). According to Reynolds (2013), a difference of  $<25\%$  between two  $K_s$  values can be considered if they refer to an ideal condition, in which measurement error, random noise, and natural

variability do not occur. The link between  $K_s$  and infiltration rate is obvious, because a given percentage difference in 3D infiltration rate at steady-state determines the same percentage difference in the calculated  $K_s$  value (Elrick & Reynolds, 1992). Consequently, an extensive value was attributed to the threshold value criterion by Reynolds (2013), meaning that differences of  $\leq 25\%$  were considered negligible, whereas differences of  $>25\%$  were deemed appreciable.

The effect of  $d$  and  $H$  on the two-term infiltration equation was then tested by applying the cumulative linearization method (Equation 2) with the first 20 min of infiltration. Performing short-duration experiments in the field is attractive to save time and water. Moreover, an experiment as short as possible is expected to justify the assumption of homogeneous soil and uniform water content in the field (Vandervaere et al., 2000a). In particular, the  $I/t^{1/2}$  vs.  $t^{1/2}$  relationship was determined for each soil (S, LS, SAL, L, and SIL), ring radius ( $r = 5, 10,$  and  $15$  cm), depth of ring insertion ( $d = 0$  and  $1$  cm), and ponded depth of water ( $H = 0$  and  $1$  cm). The linearity of the  $I/t^{1/2}$  vs.  $t^{1/2}$  relationship was assessed by the coefficient of determination,  $R^2$ , of the fitted relationship to the data. Only  $R^2$  was considered, also in accordance with Vandervaere et al. (2000a), because the data were obtained numerically and hence were free of the uncertainties typical of the laboratory and field experiments. Initially, the theoretical d0H0 scenario was considered to test linearity of the data when they were obtained in perfect agreement with the infiltration model, that is, under null  $d$  and  $H$  values. Then, the effect of  $d$  and  $H$ , both individually and in combination with each other, on the linearity of the  $I/t^{1/2}$  vs.  $t^{1/2}$  relationship and the estimated  $C_1$  and  $C_2$  values was determined.

## 4 | RESULTS AND DISCUSSION

### 4.1 | Infiltration rates and final cumulative infiltration

For all soils and both ring radii, similar  $\Delta i_r$  values were obtained during the 2 h of infiltration with the three tested

**FIGURE 1** Percentage difference,  $\Delta i_r$  (%), between the instantaneous infiltration rates,  $i_r$  [ $L T^{-1}$ ], for the d1H1 ( $d =$  ring insertion depth = 1 cm;  $H =$  ponded depth of water = 1 cm) and d0H0 ( $d = H = 0$  cm) setups for five soils (S, sand; LS, loamy sand; SAL, sandy loam; L, loam; SIL, silt loam), two ring radii ( $r = 5$  and 15 cm), and three antecedent soil water conditions (initial volumetric soil water content,  $\theta_i$ /saturated volumetric soil water content,  $\theta_s = 0.20, 0.25,$  and 0.30)

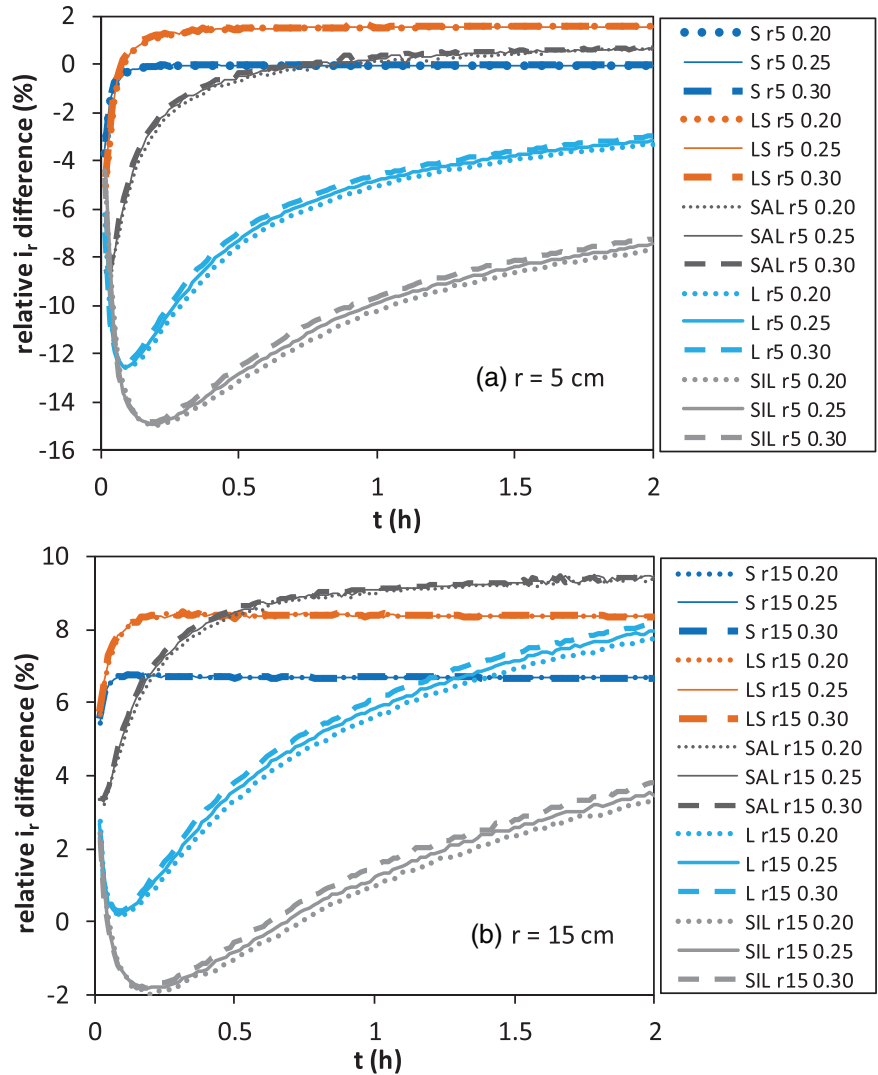


**TABLE 2** Percentage differences ( $\Delta I_{2h}$ , %) between cumulative infiltration after 2 h for the d1H1 ( $d =$  ring insertion depth = 1 cm;  $H =$  ponded depth of water = 1 cm) and d0H0 ( $d = H = 0$  cm) setups for five soils (sand [S], loamy sand [LS], sandy loam [SAL], loam [L], and silt loam [SIL]), two ring radii ( $r$ ) and three antecedent soil water conditions (initial volumetric soil water content,  $\theta_i$ /saturated volumetric soil water content,  $\theta_s = 0.20, 0.25,$  and 0.30)

Soil	$r = 5$ cm				$r = 15$ cm			
	$\theta_i/\theta_s = 0.20$	$\theta_i/\theta_s = 0.25$	$\theta_i/\theta_s = 0.30$	Largest difference	$\theta_i/\theta_s = 0.20$	$\theta_i/\theta_s = 0.25$	$\theta_i/\theta_s = 0.30$	Largest difference
	%							
S	-0.097	-0.097	-0.097	0.0002	6.68	6.69	6.68	0.01
LS	1.29	1.29	1.33	0.05	8.27	8.29	8.31	0.04
SAL	-0.71	-0.65	-0.54	0.17	8.29	8.32	8.40	0.11
L	-6.24	-6.04	-5.84	0.40	4.34	4.55	4.73	0.39
SIL	-10.4	-10.2	-10.0	0.35	0.67	0.82	0.93	0.27

$\theta_i/\theta_s$  values. In particular, three corresponding  $\Delta i_r$  values did not differ by  $>0.7\%$  for  $r = 5$  cm (Figure 1a) and 0.6% for  $r = 15$  cm (Figure 1b). A similar result was obtained for  $I_{2h}$ , because three corresponding  $\Delta I_{2h}$  values differed at the most by 0.4% with both rings, depending on the soil (Table 2). Therefore, the antecedent soil water content effect

was nearly negligible in the sense that the effect of the setup (d1H1 against d0H0) was similar for a relatively dry soil and a relatively wet one. In other terms, the detected setup effects should be rather general, at least within a range of intermediate soil water contents that represent in many circumstances the optimal conditions for

carrying out single-ring infiltration experiments in the field (Reynolds, 1993).

Taking into account that very similar results were obtained for the three considered  $\theta_i/\theta_s$  values, the subsequent data analysis was only performed with reference to the intermediate value of the three  $\theta_i/\theta_s$  ratios, that is, for  $\theta_i/\theta_s = 0.25$ .

For each soil and ring radius, the d1H0 setup yielded smaller  $i_r/K_s$  values as compared with the theoretical d0H0 setup, as shown in the three examples of Figure 2, confirming that the initial 1D stage made infiltration slower as compared with the completely unconfined process (Dušek et al., 2009) and also demonstrating that a ring insertion by only 1 cm was enough to make this slow down perceivable. On the other hand, the d0H1 setup yielded higher  $i_r/K_s$  values than the theoretical setup, because the pressure head gradient was greater in the former case (Alagna et al., 2018; Dušek et al., 2009). As expected, the normalized infiltration rates for the d1H1 setup fell into the area bounded by the curves corresponding to the d1H0 and d0H1 setups. In some cases, such as for the S soil and  $r = 5$  cm (Figure 2a), a nearly complete overlap of the infiltration rates was detected by comparing the practical (d1H1) and the theoretical (d0H0) setups. In other cases, such as for the LS soil and  $r = 15$  cm (Figure 2b), the practical experiment yielded higher  $i_r/K_s$  values than the theoretical one. In still other cases, such as for the SIL soil and  $r = 5$  cm (Figure 2c), smaller  $i_r/K_s$  values were obtained with the practical experiment than the theoretical one.

Figure 3 shows the  $\Delta i_r$  values, plotted against  $t$ , for the five soils and both the smallest and the largest tested ring ( $r = 5$  and 15 cm, respectively). The corresponding results for the intermediate ring ( $r = 10$  cm) are reported in Supplemental Figure S1. For each tested effect (ring insertion, ponded water, ring insertion, and ponded water), Table 3 lists the average of the 120  $\Delta i_r$  values corresponding to each soil and ring radius.

Using  $d = 1$  cm instead of  $d = 0$  (d1H0 vs. d0H0 setups) yielded negative  $\Delta i_r$  values in all cases, showing that the combined 1D/3D process made infiltration slower than a purely 3D process for the entire duration of the run. In particular, the 1,800 values of  $\Delta i_r$  (5 soils  $\times$  3 radii  $\times$  120  $i_r$  values for a run) varied between  $-21.8$  and  $-3.6\%$  (Figure 3; Supplemental Figure S1), and the averages of  $\Delta i_r$  ranged from  $-19.0$  to  $-5.9\%$ , depending on the soil and the ring radius (Table 3).

The instantaneous infiltration rates varied perceptibly but not substantially when the ring was inserted 1 cm into the soil. A time effect was detected for  $\Delta i_r$ . In particular, the range of the differences between the highest and the lowest value of  $\Delta i_r$  during a run varied from 1.3 percentage units (from  $-5.9$  to  $-7.2\%$ , Figure 3f) for the coarsest soil and the largest ring (S,  $r = 15$  cm) to 11.7 percentage units (from  $-10.1$  to  $-21.8\%$ , Figure 3e) for the finest soil and the smallest ring (SIL,  $r = 5$  cm). For the coarser soils (S, LS, and SAL),  $\Delta i_r$  remained essentially stable during the run except for the first minutes, in which the two considered setups ( $d = 0$  cm

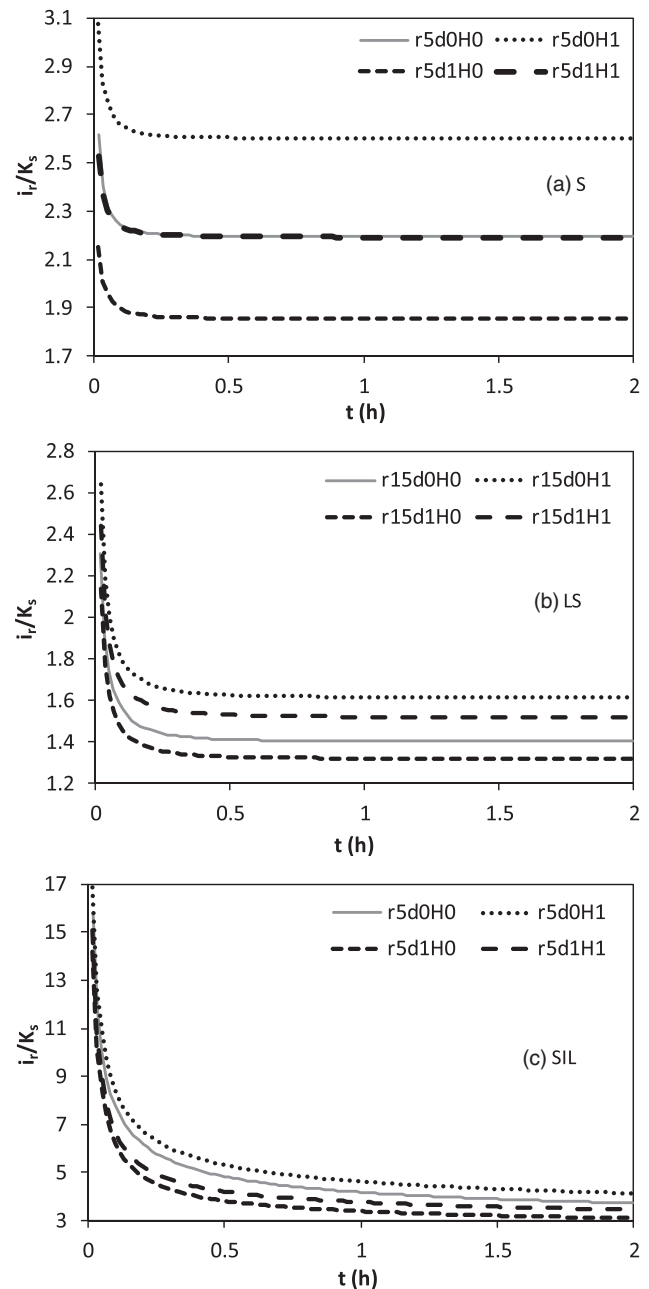


**FIGURE 2** Normalized infiltration rates,  $i_r/K_s$  ( $i_r$  = infiltration rate and  $K_s$  = saturated soil hydraulic conductivity, both in  $L T^{-1}$ ), against time,  $t$ , for the four considered setups (d0H0, d0H1, d1H0, and d1H1) differing by the ring insertion depth,  $d$  (cm), and the ponded depth of water,  $H$  (cm), and three of the considered combinations of soil and ring radius,  $r$ : (a) sandy (S) soil and  $r = 5$  cm; (b) loamy sand (LS) soil and  $r = 15$  cm; and (c) silt loam (SIL) soil and  $r = 5$  cm

and  $d = 1$  cm) differed a little more appreciably. This result appeared plausible because, in the early stage of infiltration, the differences were between a 1D and a 3D flow but later they were between a combined 1D/3D flow and a 3D flow.

After a transient phase, for the finer soils (L and SIL), the absolute differences decreased (i.e., they became less negative) by a few percentage units. However, the perception

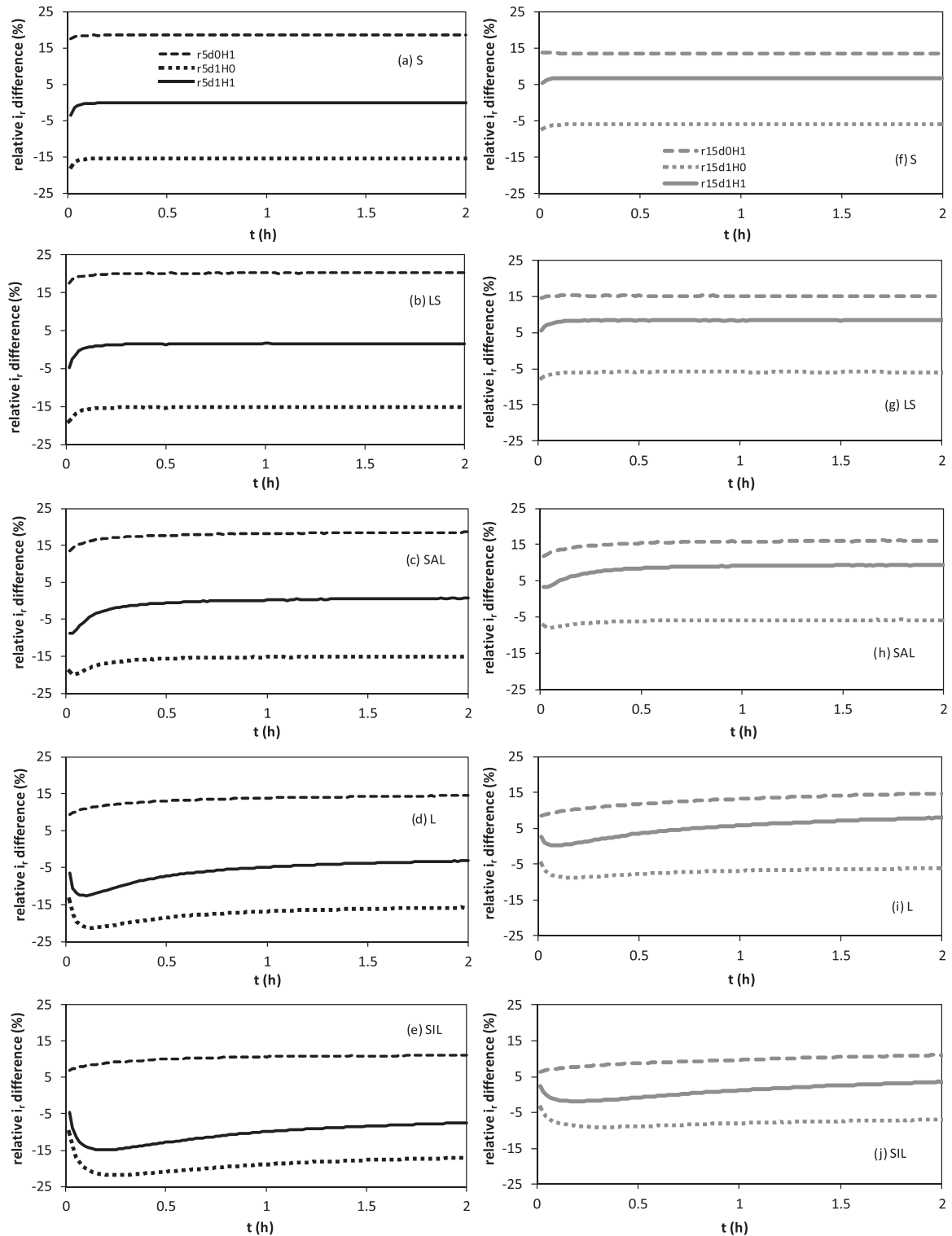


**FIGURE 3** Percentage differences,  $\Delta i_r$  (%), between the instantaneous infiltration rates,  $i_r$  [ $L T^{-1}$ ], for the d1H0, d0H1, and d1H1 setups ( $d$  = ring insertion depth = 0 or 1 cm;  $H$  = ponded depth of water = 0 or 1 cm) and the corresponding values with  $d = H = 0$  cm (d0H0 setup) for the S (sand), LS (loamy sand), SAL (sandy loam), L (loam), and SIL (silt loam) soils and two ring radii ( $r = 5$  and 15 cm) plotted against the time,  $t$ , for the 2-h infiltration experiment

was that in these soils,  $\Delta i_r$  tended to stabilize in an advanced stage of the run. The ring insertion effect on infiltration rates was a little more appreciable, with the percentage differences being more negative, as soil texture became finer, but the

soil effect was not substantial (Table 3). The averages of  $\Delta i_r$  increased with  $r$  by 9.4 to 11.1 percentage units, depending on the soil (Table 3). Therefore, the  $d$  effect decreased as the ring radius increased for all soils. Likely, as the size of the

**TABLE 3** Averages of the percentage differences ( $\Delta i_r$ , %) between the instantaneous infiltration rates ( $i_r$  [ $L T^{-1}$ ]) for the d1H0, d0H1, and d1H1 setups ( $d$  = ring insertion depth = 0 or 1 cm;  $H$  = ponded depth of water = 0 or 1 cm) and the corresponding values with  $d = H = 0$  cm (d0H0 setup) for the S (sand), LS (loamy sand), SAL (sandy loam), L (loam), and SIL (silt loam) soils and three ring radii for the 2-h infiltration experiment

Tested effect	Soil	Ring radius		
		5 cm	10 cm	15 cm
		%		
Ring insertion	S	-15.5	-8.6	-5.9
	LS	-15.4	-8.5	-5.9
	SAL	-15.6	-8.7	-6.1
	L	-17.4	-9.9	-7.0
	SIL	-19.0	-11.1	-7.9
Ponded water	S	+18.6	+15.5	+13.5
	LS	+20.1	+17.2	+15.2
	SAL	+17.9	+16.6	+15.5
	L	+13.4	+13.1	+12.9
	SIL	+10.3	+9.8	+9.5
Ring insertion and ponded water	S	-0.1	+5.4	+6.7
	LS	+1.3	+7.0	+8.3
	SAL	-0.5	+6.5	+8.6
	L	-5.8	+2.2	+5.2
	SIL	-10.4	-2.2	+1.0

ring increased, total flow from the unconfined source was less influenced by lateral divergence, and hence the differences between the two setups decreased. In other terms, the enhanced similarity between  $d = 0$  cm and  $d = 1$  cm resulted from the reduced 3D character of the flow process with a larger source.

Using  $H = 1$  cm instead of  $H = 0$  cm (d0H1 vs. d0H0 setups) yielded positive  $\Delta i_r$  values in all cases, as expected (Dohnal et al., 2016). In particular, the instantaneous  $\Delta i_r$  values varied from +6.4 to +20.3% (Figure 3; Supplemental Figure S1), and the averages of  $\Delta i_r$  varied from +9.5 to +20.1%, depending on the soil and the ring radius (Table 3). Therefore, the infiltration rates did not change substantially, based on the 25% threshold criterion used here, even with  $H$ . In almost all cases, except the S soil and  $r = 15$  cm (Figure 3f), the lowest  $\Delta i_r$  value was detected at the beginning of infiltration. The increase of  $\Delta i_r$  was small for the S and LS soils, because the range of the differences of  $\Delta i_r$  varied from 0.4 to 2.7 percentage units, depending on the soil type and  $r$  (Figure 3a,b,f,g; Supplemental Figure S1a,b). This increase was a little more appreciable for the SAL, L, and SIL soils, because the range of the differences in  $\Delta i_r$  varied by 4.3 to 6.3 percentage units in this case (Figure 3c,d,e,h,i,j; Supplemental Figure S1c,d,e). Moreover, the general perception was that  $\Delta i_r$  rapidly stabilized for the coarser soils, whereas it increased

more gradually with time for the finer soils. The averages of  $\Delta i_r$  generally decreased as the soil became finer, regardless of the ring radius, and for a given soil they decreased as  $r$  increased by a quantity varying from 5.1 percentage units for the coarser soil (S) to 0.6–0.8 percentage units for the finer soils (L and SIL) (Table 3). Therefore, the finer the soil, the smaller the effect of  $H$  on the infiltration rate. Moreover, the effect of the ring radius on the differences between the d0H1 and d0H0 setups decreased as the soil became finer. In other terms, this check suggested that a greater similarity between the two setups should be expected in the coarser soils when a large ring is used in our study. In finer soils, the ring radius became relatively less important and, in general, the small ponded depth of water did not influence infiltration significantly. A more capillarity-driven character of the infiltration process, as expected for a fine-textured soil, implies a reduced effect of the hydraulic gradient on infiltration, regardless of the ring size.

Of course, the comparison between  $d = H = 1$  cm and  $d = H = 0$  cm (d1H1 vs. d0H0 setups) yielded  $\Delta i_r$  values falling between the two extremes corresponding to the d1H0 and d0H1 setups, respectively (Figure 3; Supplemental Figure S1). Therefore, inserting the ring 1 cm into the soil reduced the tendency to obtain high  $i_r$  values as a consequence of the positive depth of ponding. Conversely, establishing this ponding condition reduced the tendency to obtain low  $i_r$  values as a consequence of ring insertion. In particular, using  $d = H = 1$  cm instead of  $d = H = 0$  cm yielded  $\Delta i_r$  values varying from -14.9 to +9.5% (Figure 3; Supplemental Figure S1) and means of  $\Delta i_r$  between -10.4 and +8.6%, depending on the soil and the ring radius (Table 3). Therefore, the infiltration rates obtained with a practical experiment (d1H1) differed from the theoretical rates (d0H0) by only a few percentage units. The averages of  $\Delta i_r$  were smallest (negative or small positive values) with the smallest ring and they increased with  $r$ , assuming positive values for all soils with the largest ring (Table 3). The ring size effect was the least noticeable for the coarsest soil (S soil, means of  $\Delta i_r$  increasing by 6.8 percentage units from  $r = 5$  cm to  $r = 15$  cm), and it increased as the soil became finer (SIL soil, means of  $\Delta i_r$  increasing by 11.5 percentage units) (Table 3). On average, the similarity between the practical and the theoretical experiment was more satisfactory with a soil-dependent ring radius. In particular, the best similarity between the two experiments was detected with a small ring for the coarse soils and a large ring for the fine soils.

For the three established comparisons between cumulative infiltration values (i.e., the d1H0, d0H1 and d1H1 setups against the d0H0 setup), Figure 4 shows the percentage differences between cumulative infiltration after 2 h against the ring radii for each soil.

Ring insertion implied naturally smaller  $I_{2h}$  values, with  $\Delta I_{2h}$  values varying from -18.3 to -5.9% (Figure 4). In particular,  $\Delta I_{2h}$  varied from -18.3% (SIL soil, Figure 4e) to



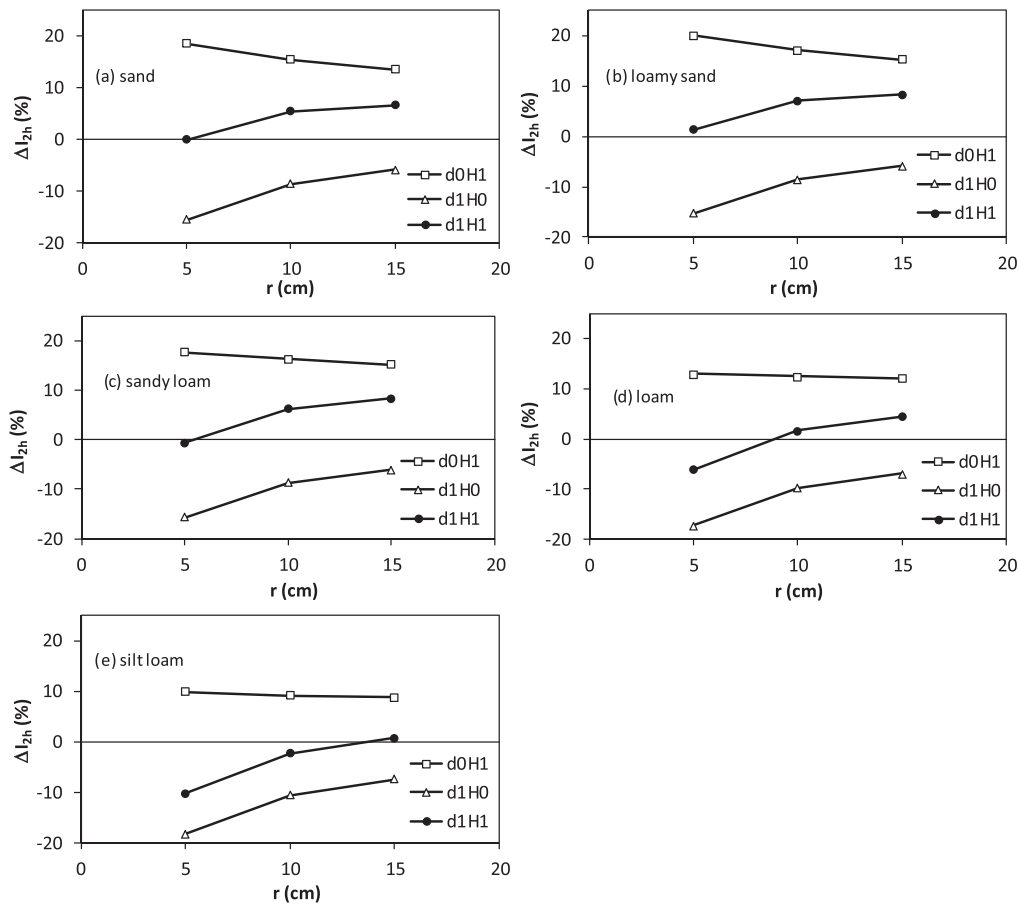


**FIGURE 4** Percentage differences,  $\Delta I_{2h}$  (%), between cumulative infiltration after 2 h for the d1H0, d0H1, and d1H1 setups ( $d$  = ring insertion depth = 0 or 1 cm;  $H$  = ponded depth of water = 0 or 1 cm) and the corresponding values with  $d = H = 0$  cm (d0H0 setup) for the five tested soils and the three ring radii,  $r$

−15.4% (LS soil, Figure 4b) for  $r = 5$  cm and from −7.4% (SIL soil, Figure 4e) to −5.9% (S soil, Figure 4a) for  $r = 15$  cm. Therefore, the decrease of  $I_{2h}$  due to ring insertion was smaller ( $\Delta I_{2h}$  values closer to zero) as the ring radius increased, and the soil did not appreciably influence  $\Delta I_{2h}$ .

Ponded water yielded higher values of cumulative infiltration, with  $\Delta I_{2h}$  values varying from +8.8 to +20.0% (Figure 4). In general, the increase of  $I_{2h}$  was greatest for the smallest ring, because  $\Delta I_{2h}$  ranged from +9.9 to +20.0%, depending on the soil, for  $r = 5$  cm and from +8.8 to +15.3% for  $r = 15$  cm. The ring size effect was more appreciable for the coarser soils than for the finer ones. In particular, the increase of  $r$  from 5 to 15 cm resulted in a decrease of  $\Delta I_{2h}$  by nearly 5 percentage units for the S and LS soils (Figure 4a,b), 2.4 units for the SAL soil (Figure 4c), and nearly 1 percentage unit for the L and SIL soils (Figure 4d,e).

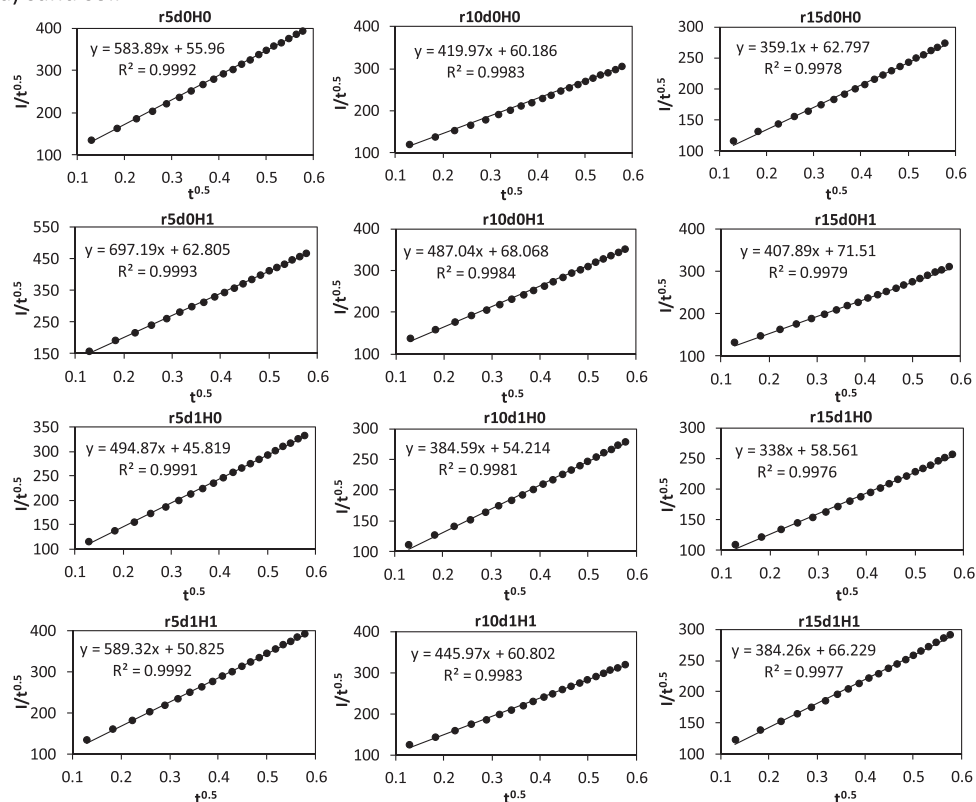
Simultaneously inserting the ring and establishing a ponded depth of water on the infiltration surface (d1H1 setup) yielded small differences overall as compared with the theoretical experiment (d0H0), because  $\Delta I_{2h}$  varied on the whole from −10.2 to +8.3% (Figure 4). For all soils,  $\Delta I_{2h}$  increased with  $r$ , and it was  $>0$  for the largest ring (from +0.8 to +8.3%).

With the smallest ring,  $\Delta I_{2h}$  was close to zero for the S, LS, and SAL soils (from −0.7 to +1.3%; Figure 4a,b,c) and negative ( $\leq -6.0\%$ ) for the L and SIL soils (Figure 4d,e). The best similarity between the practical and the theoretical experiment was detected with the smallest ring for the S, LS, and SAL soils (Figure 4a,b,c), the intermediate ring for the L soil (Figure 4d), and the largest ring for the SIL soil (Figure 4e). Therefore, the finer the soil, the larger the ring should be to obtain a similar  $I_{2h}$  value with the d0H0 and d1H1 setups.

## 4.2 | Two-parameter infiltration model

Concerning the d0H0 setup, the check of the linearity of the numerically obtained  $I/t^{1/2}$  vs.  $t^{1/2}$  data yielded  $R^2$  values that ranged from .9326 to .9992 for the five soils and the three ring radii (Table 4). As shown in Figure 5, reporting as an example the fitted relationships to the data for the coarsest (S) and the finest (SIL) soils (the corresponding results for the LS, SAL, and L soils were reported in the Supplemental Figure S2), the lowest  $R^2$  values denoted that the  $(I/t^{1/2}, t^{1/2})$  data did not describe a linear relationship for the entire duration of the run,

(a) sand soil



(b) silt loam soil

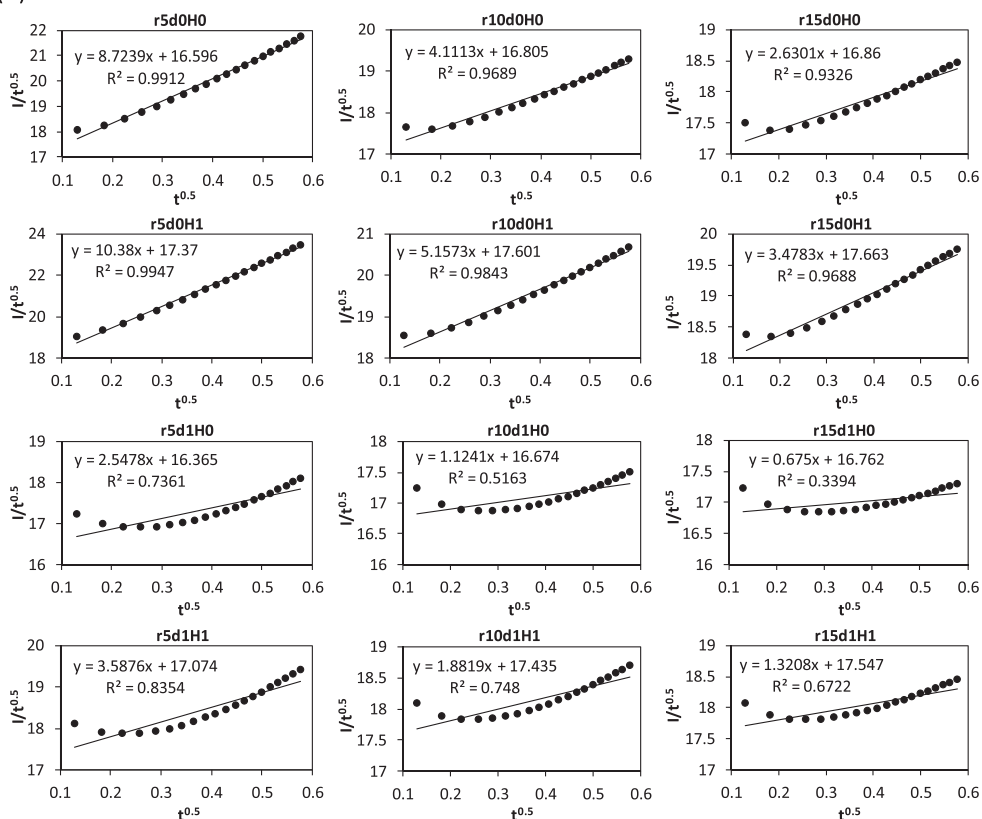


FIGURE 5 Relationship between  $I/t^{1/2}$  and  $t^{1/2}$  ( $I$  = cumulative infiltration, in mm;  $t$  = time, in h) for the infiltration data corresponding to different combinations of ring radius ( $r$  = 5, 10, and 15 cm), depth of ring insertion ( $d$  = 0 and 1 cm), and ponded depth of water ( $H$  = 0 and 1 cm): (a) sand soil and (b) silt loam soil

**TABLE 4** Intercept ( $C_1$ ), slope ( $C_2$ ), and coefficient of determination ( $R^2$ ) of the linear regression line between  $I/t^{0.5}$  and  $t^{0.5}$  (time,  $t$ , in h, infiltration,  $I$ , in mm) with reference to the tested soils (sand [S], loamy sand [LS], sandy loam [SAL], loam [L], and silt loam [SIL]) and the considered ring insertion depth ( $d$ ) and ponded depth of water ( $H$ ) combinations for each ring radius ( $r$ )

Soil	$d$	$H$	$r = 5 \text{ cm}$			$r = 10 \text{ cm}$			$r = 15 \text{ cm}$		
			$C_1$	$C_2$	$R^2$	$C_1$	$C_2$	$R^2$	$C_1$	$C_2$	$R^2$
—cm—			mm h <sup>-1/2</sup>	mm h <sup>-1</sup>	mm h <sup>-1/2</sup>	mm h <sup>-1</sup>	mm h <sup>-1/2</sup>	mm h <sup>-1</sup>	mm h <sup>-1/2</sup>	mm h <sup>-1</sup>	
S	0	0	56.0	583.9	.9992	60.2	420.0	.9983	62.8	359.1	.9978
	1	0	45.8	494.9	.9991	54.2	384.6	.9981	58.6	338.0	.9976
	0	1	62.8	697.2	.9993	68.1	487.0	.9984	71.5	407.9	.9979
	1	1	50.8	589.3	.9992	60.8	446.0	.9983	66.2	384.3	.9977
LS	0	0	45.3	258.9	.9990	47.8	180.8	.9980	49.1	152.9	.9974
	1	0	37.7	218.3	.9981	43.5	164.7	.9969	46.1	143.3	.9965
	0	1	50.5	314.8	.9991	53.8	214.3	.9981	55.6	177.7	.9977
	1	1	41.6	265.7	.9985	48.5	195.7	.9973	51.9	166.8	.9969
SAL	0	0	32.9	77.4	.9990	34.2	48.6	.9984	34.6	38.9	.9981
	1	0	28.9	60.7	.9923	31.9	41.6	.9924	33.1	34.6	.9934
	0	1	35.9	93.3	.9991	37.4	58.2	.9984	38.0	46.3	.9982
	1	1	31.1	74.6	.9938	34.7	50.6	.9937	36.1	41.7	.9942
L	0	0	20.9	19.0	.9976	21.3	10.4	.9956	21.4	7.6	.9934
	1	0	20.0	10.2	.9498	20.8	6.3	.9475	21.1	4.9	.9484
	0	1	22.3	22.5	.9983	22.8	12.5	.9969	22.9	9.3	.9957
	1	1	21.2	13.0	.9605	22.1	8.1	.9619	22.5	6.4	.9639
SIL	0	0	16.6	8.7	.9912	16.8	4.1	.9689	16.9	2.6	.9326
	1	0	16.4	2.5	.7361	16.7	1.1	.5163	16.8	0.7	.3394
	0	1	17.4	10.4	.9947	17.6	5.2	.9843	17.7	3.5	.9688
	1	1	17.1	3.6	.8354	17.4	1.9	.7480	17.5	1.3	.6722

because an upward curvature of the data points was detected in the early stages. In general,  $R^2$  decreased as the soil became finer. Moreover, an increase of the ring radius determined a decrease of  $R^2$  for all soils. Therefore, Equation 1 appropriately described the considered infiltration process for most of the considered soil and radius combinations, because the linearity of the data on the  $I/t^{1/2}$  vs.  $t^{1/2}$  plot was clearly perceivable (Smiles & Knight, 1976; Vandervaere et al., 2000a). However, the two-parameter infiltration equation did not perform well when the soil was fine textured and a large radius was used for the numerical experiment.

With reference to a 3D infiltration process, the vertical capillarity and gravity terms do not vary with the ring radius, whereas the lateral capillarity term decreases as  $r$  increases and this decrease makes infiltration slower, all other conditions being equal (Haverkamp et al., 1994; Vandervaere et al., 2000b). Therefore, this investigation suggested that a decrease of lateral capillarity had a negligible effect on the applicability of the two-parameter infiltration equation in the coarser-textured soils, because the  $I/t^{1/2}$  vs.  $t^{1/2}$  relationship remained linear even with the largest ring. In fine-textured soils, a decrease of lateral capillarity and the consequent slowdown of the process induced a nonlinearity of the relationship

between  $I/t^{1/2}$  and  $t^{1/2}$ . Therefore, for a relatively short experiment (with a duration of 20 min) sampled at a practical time interval (1 min), the curvature of the data can also be expected to occur in the theoretically most appropriate situation for applying the infiltration model by Haverkamp et al. (1994)—that is, when both  $d$  and  $H$  are null. This investigation did not prove that a data curvature does not generally occur in a coarse soil, in which infiltration should perhaps be sampled at  $<$  or  $\ll$  1-min time intervals to perceive this phenomenon. From a practical perspective, applying the infiltration model in a fine-textured soil requires using a small source to enhance lateral capillarity effects, because in this case the data better agree with Equation 2. Of course, this suggestion contrasts with the need to use sources as large as possible to improve representativeness of an individual data point (Lai & Ren, 2007).

Inserting the ring into the soil and establishing a ponded depth of water on the infiltration surface affected representation of the  $I/t^{1/2}$  vs.  $t^{1/2}$  data with a linear relationship (Table 4). In particular, the increase of  $d$  made the data less linear, whereas a higher  $H$  value improved linearity of the data (Figure 5; Supplemental Figure S2). Ring insertion had a more appreciable effect as compared with ponding water,

and both effects were appreciable only in fine-textured soils, because they appeared negligible in coarse-textured soils. In particular, ring insertion caused a decrease of  $R^2$  that did not exceed 0.7% (percentage difference between two  $R^2$  values) for the S, LS, and SAL soils but varied between 4.5 and 4.8% for the L soil, depending on  $r$ , and between 25.7 and 63.6% for SIL soil. The increase of  $R^2$  associated with a higher  $H$  value did not exceed 0.2% for the S, LS, SAL, and L soils, and it varied between 0.4 and 3.9% for the SIL soil.

A higher linearity of the  $It^{1/2}$  vs.  $t^{1/2}$  data yields more confidence about the usability of the two-parameter equation to describe the infiltration process. Therefore, increasing the pressure head a little gradient improved applicability of the infiltration equation. Instead, a process including the transition from the vertical 1D flow within the ring to 3D flow below the ring made the model less reliable, even if the ring was inserted only a little into the soil. These effects did not practically occur in coarse soils but became more perceivable and even appreciable in fine soils. A possible explanation is that as the soil becomes finer, a longer time is required for water to leave the ring and thus more sampled data points in the linear regression are affected by the presence of the ring. Consequently, the percentage of points used in the regression before water leaves the ring increases.

The theoretical setup (d0H0) generally yielded a more linear  $It^{1/2}$  vs.  $t^{1/2}$  relationship than the practical setup (d1H1) (Table 4), denoting that the decreased linearity attributable to ring insertion was not sufficiently compensated by the increased linearity due to the ponded depth of water (Figure 5; Supplemental Figure S2). The differences between the theoretical and the experimental setups were more perceivable as the soil was finer. In particular, the  $R^2$  values associated with the d1H1 setup were smaller than those associated with the d0H0 setup by no more than 0.5% for the S, LS, and SAL soils, by 3.0–3.7%, depending on  $r$ , for the L soil, and by 15.7–27.9% for the SIL soil. Therefore, the finer the soil, the more the practical experiment determined a decrease in the quality of the fitting. In a coarse soil, using  $d = H = 1$  cm instead of  $d = H = 0$  cm can be expected to have a nearly inappreciable effect on adaption of the  $It^{1/2}$  vs.  $t^{1/2}$  model to the data. However, in a fine soil, an infiltration process that could theoretically ( $d = H = 0$  cm) be described, at least approximately, by a linear relationship between the two variables (e.g., SIL soil,  $r = 5$  cm; Figure 5b) loses its linearity on the  $It^{1/2}$  vs.  $t^{1/2}$  plot if the data are collected with a practical experiment.

In this investigation, the possibility to linearize the data with reference to both the theoretical and experimental setups was recognized for the S, LS, and SAL soils (Figure 5a; Supplemental Figure S2a,b). For the L soil (Supplemental Figure S2c), the data corresponding to the theoretical setup appeared linearizable, whereas those for the experimental setup did not seem to offer this possibility. For the SIL soil (Figure 5b), the data cannot be linearized regardless of the considered

setup, with perhaps the only exception of the data obtained for  $r = 5$  cm,  $d = 0$  cm, and  $H = 0$  cm. With reference to the first three soils, a comparison was established between the  $C_1$  and  $C_2$  values obtained with the theoretical and the experimental setups. Two corresponding estimates of a parameter ( $C_1$  and  $C_2$ ) differed, in absolute value, by no more than 9.2%. Likely, this level of difference can be considered small and practically negligible in most instances, also considering that other sources of error can be identified when the experimental data are collected in the field.

Therefore, if the data obtained by a practical experiment ( $d = H = 1$  cm) can be linearized because a high  $R^2$  value is obtained by linear regression of  $It^{1/2}$  vs.  $t^{1/2}$ , then the estimates of  $C_1$  and  $C_2$  should be close to those that would be obtained with the theoretical experiment ( $d = H = 0$  cm). If the practical experiment does not yield data describing a good linear relationship between  $It^{1/2}$  and  $t^{1/2}$ , there are two possible explanations: (a) the two-parameter infiltration model does not work well even with reference to the ideal case of  $d = H = 0$  cm; or (b) it is precisely the use of  $d = H = 1$  cm instead of  $d = H = 0$  cm that precludes the possibility to linearize the data. According to this investigation, the former case is more probable in fine-textured soils, and the latter case is more probable in more intermediate soils.

## 5 | CONCLUSIONS

Infiltration experiments of the Beerkan type make use of a ring inserted a short depth into the soil, and they establish a small ponded depth of water on the infiltration surface for at least a part of the experiment. The presented numerical investigation attempted to establish if a Beerkan experiment can be used with a data analysis method that theoretically assumes a fully unconfined process under a null ponded depth of water. Examination was provided for soils ranging from a sandy soil to a silt loam soil.

In general, a perfect correspondence between the theoretical (d0H0; ring insertion depth,  $d =$  ponded depth of water,  $H = 0$  cm) and the practical (d1H1;  $d = H = 1$  cm) setup should not be expected. Inserting the ring a little into the soil reduces the instantaneous infiltration rates,  $i_t$ , for the entire run and hence cumulative infiltration,  $I$ , at the end of the process while establishing a small ponded depth of water on the infiltration surface increases  $i_t$  and  $I$ . Generally, the two effects, even if they have an opposite sign, do not compensate one with other without a residual. Differences between the two setups (d0H0 and d1H1) are, in our case, small and perhaps negligible in many practical circumstances, because they are not expected to exceed a few percentage units (approximately 10%) for both  $i_t$  and  $I$ . Moreover, these differences can also be smaller if a small ring is used for sampling coarse soils and a large ring is used in fine soils.

A similarity between the theoretical and the practical experiments with reference to the coefficients of the two-parameter infiltration model estimated by the cumulative linearization method can be expected in coarse-textured soils. In fine-textured soils, linearization of the infiltration data obtained in practice (d1H1 setup) will be more uncertain, either because the theoretical model does not work well even in the ideal condition (d0H0 setup) or because the inherent experimental uncertainties—in particular, ring insertion—deteriorate the linearity of the data.

In conclusion, this investigation, which suggests that the correspondence between the theoretical and the practical experiment should be acceptable in most of the considered circumstances, reinforced the practical interest for the Beerkan run as a practical method to collect infiltration data in the field that can then be transformed into soil hydrodynamic parameters by physically based models. Factors that could appear minor or even marginal in the context of an experimental procedure deserve specific investigations to more completely establish the limits of validity of a given assumption. Therefore, extending this investigation to a broader range of initial soil water contents and considering heterogeneous, nonrigid, and anisotropic soil conditions is advisable to reach more general conclusions. Considering soil conditions close to reality is undoubtedly important from a practical point of view. However, such simulations and their interpretation are complicated and burdened by a number of conceptual and modeling uncertainties. Reliable predictions of the behavior of a simplified system can often be useful, even for more complex cases. Different methods to collect infiltration data, such as the infiltration time of a given water volume as an alternative to fixed time intervals, should also be considered.

## ACKNOWLEDGMENTS

Michal Dohnal was supported by the Czech Science Foundation, Project no. 20-00788S. This research was partially supported by the National Natural Science Foundation of China (No. 42071038) and the Strategic Priority Research Program of the Chinese Academy of Sciences (No. XDA26040105).


## AUTHOR CONTRIBUTIONS

Vincenzo Bagarello: Conceptualization; Formal analysis; Investigation; Writing – original draft; Writing – review & editing. Michal Dohnal: Formal analysis; Investigation; Methodology; Writing – review & editing. Massimo Iovino: Formal analysis; Investigation; Methodology; Writing – review & editing. Jianbin Lai: Data curation; Investigation; Methodology; Writing – review & editing.

## CONFLICT OF INTEREST

The authors declare no conflict of interest.

## ORCID

Vincenzo Bagarello  <https://orcid.org/0000-0003-3575-549X>

Michal Dohnal  <https://orcid.org/0000-0003-1769-4750>

Massimo Iovino  <https://orcid.org/0000-0002-3454-2030>

Jianbin Lai  <https://orcid.org/0000-0002-9725-9283>

## REFERENCES

- Alagna, V., Bagarello, V., Cecere, N., Concialdi, P., & Iovino, M. (2018). A test of water pouring height and run intermittence effects on single-ring infiltration rates. *Hydrological Processes*, 32, 3793–3804. <https://doi.org/10.1002/hyp.13290>
- Bagarello, V., Iovino, M., & Lai, J. (2019). Accuracy of saturated soil hydraulic conductivity estimated from numerically simulated single-ring infiltrations. *Vadose Zone Journal*, 18, 180122. <https://doi.org/10.2136/vzj2018.06.0122>
- Carsel, R. F., & Parrish, R. S. (1988). Developing joint probability distributions of soil water retention characteristics. *Water Resources Research*, 24, 755–769. <https://doi.org/10.1029/WR024i005p00755>
- Di Prima, S. (2015). Automated single ring infiltrometer with a low-cost microcontroller circuit. *Computer and Electronics in Agriculture*, 118, 390–395. <https://doi.org/10.1016/j.compag.2015.09.022>
- Dohnal, M., Vogel, T., Dusek, J., Votrubova, J., & Tesar, M. (2016). Interpretation of ponded infiltration data using numerical experiments. *Journal of Hydrology and Hydromechanics*, 64, 289–299. <https://doi.org/10.1515/johh-2016-0020>
- Dušek, J., Dohnal, M., & Vogel, T. (2009). Numerical analysis of ponded infiltration experiment under different experimental conditions. *Soil & Water Research*, 4, S22–S27. <https://doi.org/10.17221/1368-SWR>
- Elrick, D. E., & Reynolds, W. D. (1992). Methods for analyzing constant-head well permeameter data. *Soil Science Society of America Journal*, 56, 320–323. <https://doi.org/10.2136/sssaj1992.03615995005600010052x>
- Haverkamp, R., Ross, P. J., Smettem, K. R. J., & Parlange, J. Y. (1994). Three-dimensional analysis of infiltration from the disc infiltrometer. 2. Physically-based infiltration equation. *Water Resources Research*, 30, 2931–2935. <https://doi.org/10.1029/94WR01788>
- Hoefner, K., Beylich, A., Chabbi, A., Cluzeau, D., Dascalu, D., Graefe, U., Guzmán, G., Hallaire, V., Hanisch, J., Landa, B. B., Linsler, D., Menasseri, S., Öpik, M., Potthoff, M., Sandor, M., Scheu, S., Schmelz, R. M., Engell, I., Schrader, S., & Pérès, G. (2021). Legacy effects of temporary grassland in annual crop rotation on soil ecosystem services. *Science of the Total Environment*, 780, 146140. <https://doi.org/10.1016/j.scitotenv.2021.146140>
- Lai, J., Luo, Y., & Ren, L. (2010). Buffer index effects on hydraulic conductivity measurements using numerical simulations of double-ring infiltration. *Soil Science Society of America Journal*, 74, 1526–1536. <https://doi.org/10.2136/sssaj2009.0450>
- Lai, J., & Ren, L. (2007). Assessing the size dependency of measured hydraulic conductivity using double-ring infiltrometers and numerical simulation. *Soil Science Society of America Journal*, 71, 1667–1675. <https://doi.org/10.2136/sssaj2006.0227>
- Lassabatere, L., Angulo-Jaramillo, R., Soria Ugalde, J. M., Cuenca, R., Braud, I., & Haverkamp, R. (2006). Beerkan estimation of soil transfer parameters through infiltration experiments—BEST. *Soil Science Society of America Journal*, 70(2), 521–535. <https://doi.org/10.2136/sssaj2005.0026>

- Lozano-Baez, S. E., Domínguez-Haydar, Y., Di Prima, S., Cooper, M., & Castellini, M. (2021). Shade-grown coffee in Colombia benefits soil hydraulic conductivity. *Sustainability*, *13*, 7768. <https://doi.org/10.3390/su13147768>
- Mualem, Y. (1976). A new model for predicting the hydraulic conductivity of unsaturated porous media. *Water Resources Research*, *12*, 513–522. <https://doi.org/10.1029/WR012i003p00513>
- Philip, J. R. (1957). The theory of infiltration: 4. Sorptivity and algebraic infiltration equations. *Soil Science*, *84*, 257–264. <https://doi.org/10.1097/00010694-195709000-00010>
- Reynolds, W. D. (1993). Chapter 56. Saturated hydraulic conductivity: Field measurement. In Carter, M. R. (Ed.), *Soil sampling and methods of analysis* (pp. 599–613). Canadian Society of Soil Science.
- Reynolds, W. D. (2013). An assessment of borehole infiltration analyses for measuring field-saturated hydraulic conductivity in the vadose zone. *Engineering Geology*, *159*, 119–130. <https://doi.org/10.1016/j.enggeo.2013.02.006>
- Šimůnek, J., Šejna, M., & van Genuchten, M. Th. (2007). *The HYDRUS software package for simulating two-and three-dimensional movement of water, heat, and multiple solutes in variably-saturated media* (Technical Manual, Version 1.0). PC Progress.
- Šimůnek, J., van Genuchten, M. Th., & Sejna, M. (2016). Recent developments and applications of the HYDRUS computer software packages. *Vadose Zone Journal*, *15*(7), <https://doi.org/10.2136/vzj2016.04.0033>
- Smiles, D. E., & Knight, J. H. (1976). A note on the use of the Philip infiltration equation. *Australian Journal of Soil Research*, *14*, 103–108. <https://doi.org/10.1071/SR9760103>
- Touma, J., Voltz, M., & Albergel, J. (2007). Determining soil saturated hydraulic conductivity and sorptivity from single ring infiltration tests. *European Journal of Soil Science*, *58*(1), 229–238. <https://doi.org/10.1111/j.1365-2389.2006.00830.x>
- Vandervaere, J.-P., Vauclin, M., & Elrick, D. E. (2000a). Transient flow from tension infiltrometers: I. The two-parameter equation. *Soil Science Society of America Journal*, *64*, 1263–1272. <https://doi.org/10.2136/sssaj2000.6441263x>
- Vandervaere, J.-P., Vauclin, M., & Elrick, D. E. (2000b). Transient flow from tension infiltrometers: II. Four methods to determine sorptivity and conductivity. *Soil Science Society of America Journal*, *64*, 1272–1284. <https://doi.org/10.2136/sssaj2000.6441272x>
- van Genuchten, M. Th. (1980). A closed-form equation for predicting the hydraulic conductivity of unsaturated soils. *Soil Science Society of America Journal*, *44*(5), 892–898. <https://doi.org/10.2136/sssaj1980.03615995004400050002x>
- Varvaris, I., Pittaki-Chrysodonta, Z., Børgesen, C. D., & Iversen, B. V. (2021). Parameterization of two-dimensional approaches in HYDRUS-2D. Part 1: For simulating water flow dynamics in catchment scale. *Soil Science Society of America Journal*, *85*, 1578–1599. <https://doi.org/10.1002/saj2.20307>
- Wu, L., Pan, L., Roberson, M. J., & Shouse, P. J. (1997). Numerical evaluation of ring-infiltrometers under various soil conditions. *Soil Science*, *162*, 771–777. <https://doi.org/10.1097/00010694-199711000-00001>
- Wu, L., Swan, J. B., Nieber, J. L., & Allmaras, R. R. (1993). Soil-macropore and layer influences on saturated hydraulic conductivity measured with borehole permeameters. *Soil Science Society of America Journal*, *57*, 917–923. <https://doi.org/10.2136/sssaj1993.03615995005700040006x>
- Xu, X., Lewis, C., Liu, W., Albertson, J. D., & Kiely, G. (2012). Analysis of single-ring infiltrometer data for soil hydraulic properties estimation: Comparison of BEST and Wu methods. *Agricultural Water Management*, *107*, 34–41. <https://doi.org/10.1016/j.agwat.2012.01.004>

## SUPPORTING INFORMATION

Additional supporting information can be found online in the Supporting Information section at the end of this article.

**How to cite this article:** Bagarello, V., Dohnal, M., Iovino, M., & Lai, J. (2022). Correspondence between theory and practice of a Beerkan infiltration experiment. *Vadose Zone Journal*, *21*, e20220. <https://doi.org/10.1002/vzj2.20220>